THE LOCATION OF Mn^{2+} IONS IN ZnO:Mn NANOCRYSTALS SYNTHESIZED BY ULTRASONIC AEROSOL PYROLYSIS

O. V. Kovalenko*, V. Yu. Vorovsky, V. V. Slavnyi

Oles Honchar Dnipro National University, Dnipro, Ukraine
**e-mail: kovalenko.dnu@gmail.com*

The paper presents the results of EPR studies of ZnO:Mn nanocrystals with an impurity concentration of 2 at.% obtained by ultrasonic pyrolysis of aerosol. It is shown that under non-equilibrium conditions of synthesis by this method, Mn^{2+} impurity ions are unevenly distributed in the volume of the nanocrystal, and the nanocrystal itself has a defective surface layer. Mn^{2+} ions located in this surface layer, together with oxygen vacancies, determine the ferromagnetic properties of the sample. Significant thermal stability of the defective surface layer is established during heat treatment of the sample at T=550°C for 1 hour. The possibility of restoring the ferromagnetic properties of ZnO:Mn nanocrystals by heat treatment in hydrogen is established. Such treatment restores the concentration of oxygen vacancies in the surface layer, which are lost during the previous heat treatment in air.

Keywords: method of ultrasonic aerosol pyrolysis, oxygen vacancies, X-ray diffraction analysis, Mn^{2+} ions, ferromagnetic properties, heat treatment, ferromagnetic properties.

Received 17.10.2025; Received in revised form 25.11.2025; Accepted 10.12.2025

1. Introduction

Diluted magnetic semiconductors (DMS) were the focus of attention for a long time due to their potential use in spintronics devices [1]. It is known that the ferromagnetic properties (FP) of such materials arise as a result of electron-spin interaction between the sp-orbitals of the semiconductor matrix atoms and the 3d-orbitals of the impurity atoms [2]. One of the promising DMS is manganese-doped zinc oxide – ZnO:Mn [3]. Among all transition element atoms, the Mn atom is the most promising – in the Mn^{2+} valence state, it has five unpaired electrons in the $3d^5$ orbit. This determines its high efficiency in magnetic interaction. In addition, the ionic radius of the Mn^{2+} ion does not differ significantly from the ionic radius of the Zn^{2+} ion, which makes it possible to achieve high solubility of the impurity when doping ZnO. Therefore, the achievement of high magnetic characteristics of ZnO:Mn nanocrystals (NCs) was associated with an increase in the concentration of Mn^{2+} ions in ZnO. However, studies show that there are critical values of Mn concentration (from 2 to 4 at. %), at which ZnO:Mn NCs, regardless of the synthesis method, have maximum magnetization [4]. Further doping leads to a decrease in the FP of the samples. It has been established that the reason for this is the inhomogeneous distribution of Mn impurities in the NC volume. Recent DMS studies show that intrinsic defects in the crystal lattice (CL) also play a decisive role in the formation of FPs [5]. The defective state in ZnO:Mn NCs occurs under non-equilibrium, short-term synthesis conditions, mainly at low temperatures T < 600ºC [6]. In addition, it is established that under non-equilibrium conditions of ZnO:Mn NC synthesis, a significant part of Mn atoms accumulates on the surface of the NC [7]. The nature of this phenomenon is explained by the peculiarities and kinetics of their growth from a supersaturated solution by the method of ultrasonic aerosol pyrolysis (UAP) [8]. At the initial stage of growth, NCs are formed from the atoms of the main substance, which increases the concentration of the impurity in the solution around the NC. This results in the formation of a structurally perfect, defect-free NC core. At the final stage of growth, the NC is formed from a more diluted solution, which leads to the appearance of CL defects in its surface layer (SL). At the same time, the appearance of an impurity atom on the crystal plane of the NC stops its growth in this crystallographic direction and contributes to the further accumulation of impurities on this plane, which, in turn, increases their concentration on the surface of the NC.

Work [9] demonstrates the existence of a heterogeneous crystal structure of ZnO:Mn (2 at.%) in the form of a defect-free core and a defective shell. It has been established that the ultra-fine structure (UFS) lines of the EPR spectrum of this sample consist of a superposition of two spectra, SI and SII. The SI spectrum is caused by Mn^{2+} ions located in the core of the NC and isovalently replacing Zn^{2+} ions in the ZnO lattice nodes. The SII spectrum is associated with Mn^{2+} ions located in the defective SL [7]. A similar doubling of the UFS lines of the EPR spectrum was also observed in [10]. In [7], the effect of heat treatment (HT) on the SII spectrum lines in the range from T = 100ºC to T = 500ºC was investigated. It is important to note that information about the intensity of the SII spectrum line indicates the concentration of Mn^{2+} ions in the defective SL. Studies of the PL spectra [9, 11] of ZnO:Mn NC samples showed that a large number of oxygen vacancies (V_o) are concentrated on the surface of the NC. According to the bound magnetic polarons (BMP) model [2], the presence of intrinsic V_o defects and Mn^{2+} ions in the defective SL may cause the appearance of FP and become the basis for the presence of 'surface' ferromagnetism in NCs [12]. Thus, it was established that during non-equilibrium synthesis, Mn^{2+} impurity ions are unevenly distributed in the volume of ZnO:Mn NCs, and the part of them, on which the FP depends, is located in the defective SL. Therefore, studying the conditions for the formation of defective SL in ZnO:Mn NCs obtained by the UPA method is a relevant task. Information about the distribution of Mn^{2+} impurity ions in ZnO:Mn NCs during non-equilibrium synthesis will allow us to create a model of effective doping and to control the FP of the samples.

2. Method of synthesis of NC ZnO:Mn

We studied samples of ZnO:Mn with a Mn impurity concentration of 2 at. % obtained by the UAP method. The method is based on the thermal decomposition of aerosol droplets of the initial solution as they pass through the thermal zone [13]. In this case, thermal decomposition occurs in the carrier gas atmosphere, and the final product is separated on a mesh filter heated to the appropriate temperature. For the synthesis of NC ZnO:Mn using this method, an aqueous solution of zinc nitrate $Zn(NO_3)_2 \cdot 6H_2O$ with a concentration of 0.3 M was used. The required amount of manganese nitrate $Mn(NO_3)_2 \cdot 6H_2O$ was added to the base solution of zinc nitrate. During synthesis, air was used as the carrier gas, the solution flow rate was 20 l/h, the synthesis temperature was T = 550ºC, and the duration of the solution's stay in the thermal zone was 6 ÷ 8 s. Due to the fact that synthesis by this method takes place in a microdrop with a size of D = 1.0 ÷ 2.0 μm, the influence of external factors is reduced as it passes through the thermal zone of the furnace, which allows a pure final synthesis product to be obtained.

The obtained ZnO:Mn samples were subjected to heat treatment in air at temperatures of T = 550°C and T = 850°C for 20 minutes, as well as heat treatment at a temperature of T = 550°C for 1 hour. The samples were cooled in the cold zone of the furnace for 15 minutes in a stream of gaseous nitrogen.

3. Research of NCs ZnO:Mn using EPR and their analysis

The samples were studied using the EPR method on a RADIOPAN SE/X 25433 radio spectrometer in the centimeter wavelength range at a frequency of 9.3 GHz. When obtaining EPR spectra, all samples were studied under the same spectrometer operating conditions and were normalized by mass. This made it possible to conduct a comparative analysis of the spectra by intensity.

The study of defective SL was carried out by analyzing the UFS lines of the EPR spectrum of ZnO:Mn samples. Among the methods for studying the crystal structure of DMS, the EPR method has certain advantages due to its high resolution and sensitivity. This method makes it possible to obtain information about the local environment of the impurity ion, as well as to determine the position of ions in the crystal lattice, which allows it to be used for studying the process of doping ZnO with Mn impurity [14]. The EPR method also allows detecting the presence of ferromagnetic clusters in samples, which manifests itself in the appearance of a ferromagnetic resonance (FMR) line in the EPR spectrum of samples in the low magnetic field region [15].

Fig. 1a shows the EPR spectrum of the ZnO:Mn sample. In this spectrum, in the region of magnetic field induction values H = 300 ÷ 350 mT, there is a line of Mn^{2+} ions (spectra SI and SII), which, in turn, consist of six lines. The SI spectrum is caused by Mn^{2+} ions located at the nodes of the ZnO nanocrystals. The intensity of these lines allows us to draw conclusions about the effectiveness of the doping process of ZnO:Mn NC with Mn impurity. The SII spectrum is associated with Mn^{2+} ions located in the defective SL. The intensity of these lines allows us to draw conclusions about the value of the FP of the sample. This spectrum is our research subject. The UFS lines of Mn^{2+} ions overlap a broad background absorption line (2 in Fig. 1a), which is caused by the dipole-dipole interaction between Mn^{2+} ions located between the nodes of the ZnO crystal lattice. These ions form paramagnetic clusters and determine the paramagnetic properties of the samples [16]. At a significant impurity concentration, such interaction between Mn^{2+} ions leads to the appearance of antiferromagnetic properties in the samples [2]. Also, in the EPR spectrum in the region of low magnetic field values H ~ 250 mT, a broad, unstructured FMR line is registered, which is caused by the presence of ferromagnetic clusters in the sample and is a sign of the sample's FP [15]. It is known that FP is caused by Mn^{2+} ions located in a defective SL.

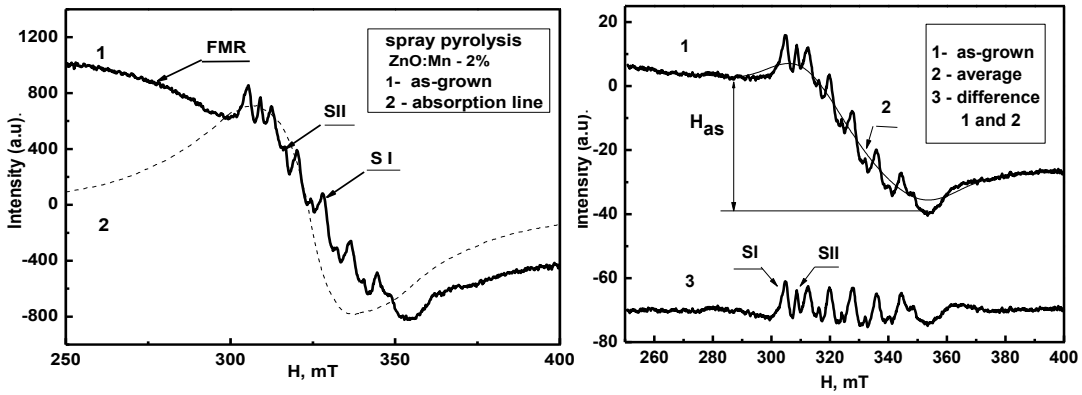

a b

Fig. 1. Structure of the EPR spectrum of ZnO:Mn, consisting of FMR lines, SI and SII spectra of Mn^{2+} ions, which together form the experimental lines (1), (2): (a) background absorption line; (b) separation of SI and SII spectrum lines (3) by finding the difference between the experimental spectrum (1) and its averaging line (2), H_{as} – EPR spectrum asymmetry parameter.

Thus, the appearance of ferromagnetic, paramagnetic or antiferromagnetic properties in the sample depends on the position of Mn^{2+} ions in the CL and in the volume of the ZnO:Mn NC.

The SI and SII spectra (3) were studied by graphically separating these spectra based on the difference between the experimental EPR spectrum (1) and the averaging line (2)

obtained using the Origin software package (Fig. 1b). This made it possible to obtain Mn^{2+} ion UFS lines in a better form for further analysis. This research method was used in [7]. In [17], the integral area of six peaks of the UFS line of the SI spectrum was calculated, which made it possible to estimate the concentration of Mn^{2+} ions located at the nodes of the ZnO:Mn nanocrystals. It was shown that, compared to the total concentration of Mn^{2+} ions (at 2 at.% the value of $C_{Mn} = 1.49 \cdot 10^{20}$ 1/g), the concentration of Mn^{2+} nodal ions does not exceed 0.15%. This indicates the low efficiency of the process of doping ZnO with Mn impurity under non-equilibrium conditions of synthesis by the UPA method. Most Mn^{2+} ions occupy an interstitial position in the crystal lattice, which manifests itself in a significant asymmetry of the EPR spectrum (the asymmetry parameter H_{as} in Fig. 1b) and determines the paramagnetic properties of the samples. The rest of these ions are located in the FP, form the SII lines of the EPR spectrum and determine the FP. Mn atoms can also be found in the amorphous intercrystalline medium, since not all the solution mass can undergo thermal decomposition during the short synthesis time.

We investigated the effect of different HT modes in air on the defective SL of the ZnO:Mn sample. From the EPR spectra of the synthesized sample after HT at T = 550°C and T = 850°C (Fig. 2a), it can be concluded that with an increase in the TO time at T = 550°C, the intensity of the SII spectrum lines practically does not decrease, but heat treatment at T = 850°C for 20 min. leads to its disappearance. A more detailed analysis of the UFS lines of the EPR spectra of Mn^{2+} ions obtained by the separation method (Fig. 2b) allowed us to determine the values of the amplitudes of the first peak (AI, AII) in the EPR spectra SI and SII, as well as the asymmetry parameter H_{as} of the spectra in the ZnO:Mn samples Mn after HT (Table 1).

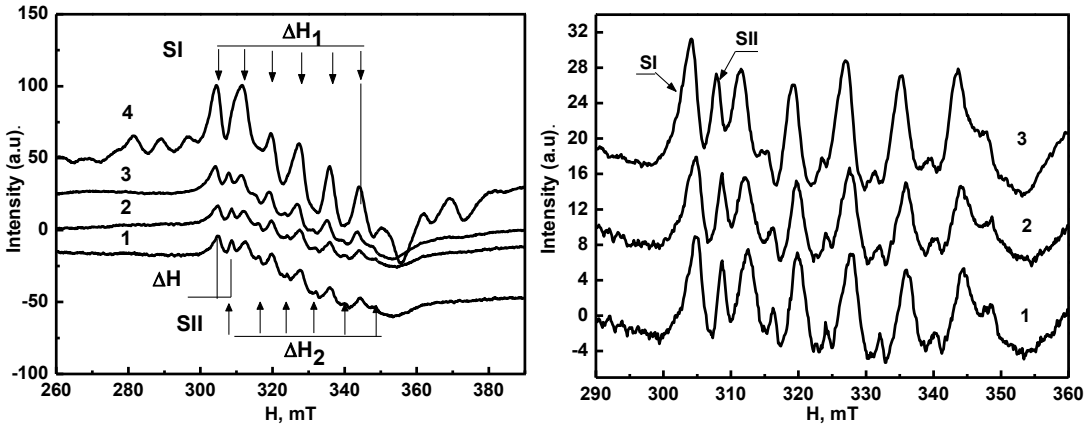

a b

Fig. 2. EPR spectra of ZnO:Mn samples:
(a): (1) synthesized sample; after HT: (2) at T = 550°C (20 min.), (3) at T = 550°C (1 h.), (4) at T = 850°C (20 min.);
(b): separate EPR spectra of SI and SII after HT: (1) at T = 550°C (20 min.), (2) at T = 550°C (1 h.), (3) at T = 850°C (20 min.).

The asymmetry parameter H_{as} of spectra after long-term HT (1 hour) at low temperature (T = 550°C), as well as after short-term HT (20 minutes) at high temperature (T = 850°C) increases. A slight decrease in the asymmetry parameter H_{as} of the spectrum in the sample after HT at T = 550°C for 20 min. may be due to the fact that during such HT secondary

MnO_2 phases arise in the sample [9, 19], and a certain amount of Mn atoms are spent on their formation.

From the analysis of the EPR spectra (Fig. 2a), it can be concluded that the shift between the SI and SII spectral lines is $\Delta H = 3.7$ mT. The width of the SI line is $\Delta H_1 = 39.25$ mT, and the hyperfine interaction constant is $A_1 = 7.85$ mT. This value of the constant A_1 corresponds to the tetrahedral environment of Mn^{2+} ions in the ZnO crystal lattice. The width of the SII line is $\Delta H_2 = 39.85$ mT, and the constant $A_2 = 7.96$ mT. It can be assumed that Mn^{2+} ions located on the surface of the NC are also in a tetrahedral environment.

Table 1

Parameters of the UFS lines of the EPR spectra of Mn^{2+} ions in the EPR spectra of SI and SII in ZnO:Mn: values of the amplitudes of the first peak (AI, AII) in the EPR spectra of SI, SII, the asymmetry parameter H_{as} of the spectra

Samples of ZnO:Mn (2 at.%)	Asymmetry	Intensity	
	H_{as}	AI, a.u.	AII, a.u.
Synthesized	38,3	12,4	6,5
HT at T = 550°C, (20 min.)	25,8	9,4	5,3
HT at T = 550°C, (1 hour)	44,2	12,2	6,1
HT at T = 850°C, (20 min.)	64,5	36,4	0

4. Conclusions

The studies showed significant thermal stability of the EPR lines of the SII spectrum during HT at T = 550°, since the intensity of the peaks of this spectrum changes little. This indicates that the concentration of Mn^{2+} ions in the defective SL also changes little. At the same time, in [9], it was shown that the FP of the ZnO:Mn sample after short-term (20 min) HT at T = 550°C in air decreases: the value of the specific magnetization M_s changes from 0.028 emu/g to 0.011 emu/g). This is explained by the fact that during such heat treatment, the number of oxygen vacancies V_o in the defective SL significantly decreases. However, as shown in [20], their number can be restored by heat treatment of the sample in hydrogen at T = 550°C for 20 min. The magnetization of the sample thereby increases to $M_s = 0.023$ emu/g. Hydrogen restores the concentration of oxygen vacancies V_o in the SL, which were lost during the previous HT in air. This, in turn, creates conditions for the restoration of the FP.

References

1. **Žutić, I.** Bipolar spintronics: fundamentals and applications / I. Žutić, J. Fabian, S. C. Erwin // IBM J. Res. Dev. – 2006. – Vol. 50, No. 1. – P. 121 – 139.

2. **Coey, J. M. D.** Donor impurity band exchange in dilute ferromagnetic oxides / J. M. D. Coey, M. Venkatesan, C. B. Fitzgerald // J. Nat. Mater. – 2005. – Vol. 4. – P. 173 – 179.

3. **Dietl, T.** Zener model description of ferromagnetism in zinc-blende magnetic semiconductors / T. Dietl, H. Ohno, F. Matsukura, J. Cibert, D. Ferrand // Science. – 2000. – Vol. 287, Issue 5455. – P. 1019 –1022.

4. **Sharma, P.** Ferromagnetism above room temperature in bulk and transparent thin films of Mn-doped ZnO / P. Sharma, A. Gupta, K. Rao. et al. // J. Nature Materials. – 2003. – No. 2 (10). – P. 673-7.

5. **Ekhande, L. V.** Role of defects in enhancing room temperature ferromagnetism of Mn doped ZnO nanoparticles / L. V. Ekhande, V. V. Dhas, Y. D. Kolekar, et al. // Phys. Status Solidi B. – 2013. – Vol. 250, No.7. – P. 1389 – 1397.

6. **Kovalenko, O. V.** Peculiarities of doping of ZnO:Mn nanocrystals during their synthesis by the aerosol pyrolysis method / O. V. Kovalenko, V. Yu. Vorovsky, O. V. Khmelenko, Ye. G. Plakhtii // J. Physics and Electronics. – 2020. – Vol. 28(2). – P. 91 – 94.

7. **Zhou, H.** Magnetic resonance investigation of Mn^{2+} in ZnO nanocrystals / H. Zhou, D. M. Hofmann, A. Hofstaetter et al. // J. Appl. Phys. – 2003. – Vol. 94, No. 3. – P. 1965 – 1968.

8. **Layek, A.** A Generalized Three-Stage Mechanism of ZnO Nanoparticle Formation in Homogeneous Liquid Medium / A. Layek, G. Mishra, A. Sharma, et al. // J. Phys. Chem. C. – 2012. – Vol. 116, No. 46. – P. 24757 – 24769.

9. **Kovalenko, O. V.** The effect of heat treatment on the magnetic properties of ZnO:Mn nananocrystals obtained by ultrasonic spray pyrolysis / O. V. Kovalenko, V. Yu. Vorovsky, O. V. Khmelenko // J. Functional Materials. – 2020. – Vol. 27, No. 4. – P. 687 – 694.

10. **Romeiro, F. C.** Photoluminescence and Magnetism in Mn^{2+}-Doped ZnO Nanostructures Grown Rapidly by the Microwave Hydrothermal Method / F. C. Romeiro, J. Z. Marinho, et al. // J. Phys. Chem. C. – 2013. – Vol. 117, No. 49. – P. 26222 – 26227.

11. **Zhan, P.** Oxygen vacancy–induced ferromagnetism in un-doped ZnO thin films / P. Zhan**,** W. Wang, C. Lui, et al. // J. Appl. Phys. – 2012. – Vol. 111, No. 3. – P. 033501 – 033505.

12. **Kovalenko, O. V.** Dependence of Magnetic Properties of ZnO:Mn Nanocrystals on Synthesis Conditions / O. V. Kovalenko, V. Yu. Vorovsky // J. Nano. Electron. Phys. – 2022. – Vol. 3. – P. 03030-1-03030-5.

13. **Tsai, S. C.** Ultrasonic spray pyrolysis for nanoparticles synthesis / S. C. Tsai. // J. Mater. Sci. – 2004. – Vol. 39, No. 11. – P. 3647 – 3657.

14. **Kaftelen, H.** EPR and photoluminescence spectroscopy studies on the defect structure of ZnO nanocrystals / H. Kaftelen, K. Ocakoglu, R. Thomann, et al. // J. Phys. Rev. B. – 2012. – Vol. 86. – P. 014113.

15. **Toloman, D.** Evidence by EPR of ferromagnetic phase in Mn-doped ZnO nanoparticles annealed at different temperatures / D. Toloman, A. Mesaros, A. Popa, et al. // Journal of Alloys and Compounds. – 2013. – Vol. 551. – P. 502 – 507.

16. **Phan, T. L.** Local structure and paramagnetic properties of $Zn_{1-x}Mn_xO$ / T. L. Phan, P. Zhang, D. S. Yang, et al. // J. Appl. Phys. – 2011. – Vol. 110, Issue 6, 063912. – P. 1 – 6.

17. **Kovalenko, O. V.** Magnetic moment of Mn^{2+} ions that are responsible for the ferromagnetic properties of ZnO:Mn nanocrystals / O. V. Kovalenko, V. Yu. Vorovsky // J. Phys. Chem. Solid St. – 2023. Vol. 24, No. 4. – P. 650 – 655.

18. **Kovalenko, O. V.** Crystal structure of ZnO nanocrystals synthesized by the spray pyrolysis method / O. V. Kovalenko, V. V. Slavnyi // J. Physics and Electronics. – 2023. – Vol. 31(2). – P. 67 – 72.

19. **Zhang, J.** Sample preparation and annealing effects on the ferromagnetism in Mn-doped ZnO / J. Zhang, R. Skomski, D. J. Sellmyer // J. Appl. Phys. – 2005. – Vol. 97, Issue 10, 10D303.

20. **Kovalenko, O. V.** Effect of short-term heat treatment in the hydrogen on magnetic properties of ZnO:Mn nanocrystals / O. V. Kovalenko, V. Yu. Vorovsky, O. V. Khmelenko, O. I. Kushnerov // J. Phys. Chem. Solid St. – 2022. – Vol. 23, No. 3. – P. 569 – 574.